INTERNATIONAL JOURNAL OF LATEST TECHNOLOGY IN ENGINEERING, MANAGEMENT & APPLIED SCIENCE (IJLTEMAS)

ISSN 2278-2540 | DOI: 10.51583/IJLTEMAS | Volume XIII, Issue V, May 2024

Transesterification of Castor Oil for Biodiesel Production Using H_2SO_4 Wet Impregnated Snail, Egg and Crab Shell Catalyst.

***Nwanekwu Akunna Maureen, *Okoye Patrice-Anthony Chudi, Vincent Ishmael Egbulefu Ajiwe, Omuku Patrick Enuneku, Onyeije Ugomma Chibuzor.**

Department of Pure and Industrial Chemistry, Nnamdi Azikiwe University, Awka, Nigeria.

***Corresponding Author**

DOI : https://doi.org/10.51583/IJLTEMAS.2024.130520

Received: 19 May 2024; Accepted: 28 May 2024; Published: 21 June 2024

Abstract: Biodiesel does not only provide a sustainable alternative for diesel fuel but also enables the transformation and utilization of wastes into high value products. Therefore, the aim of this study is to use heterogeneous catalysts derived from wet-impregnated snail, crab and egg shell waste in the production of biodiesel using castor oil. The use of castor oil as the preferred non-edible oil is due its high ricinoleic acid concentration as well as its high solubility in alcohol. The uncalcined egg, snail and crab shell catalysts were identified as E, S and C respectively while $CS_{800}{}^{o}{}_{C}/H_2SO_4$, $CC_{900}{}^{o}{}_{C}/H_2SO_4$, and $CE_{900}{}^{o}{}_{C}/H_2SO_4$ represents calcined/impregnated snail, crab and egg shell catalysts respectively. The BET and SEM were used to determine the surface morphology and microstructure of the catalysts while the structure of the crystalline materials and the elemental composition of the catalysts were determined using the XRD and XRF respectively. GC-MS was used to analyze the free fatty acid composition of the oil and FTIR to obtain the organic and polymeric materials present. The physical and chemical analysis of the crude castor oil was carried out so as to determine the percentage of FFA contained in the oil. Each of the calcined/impregnated snail, crab and egg shells were reacted singly with castor oil in the biodiesel production where CS, CC and CE are acronyms that stands for castor oil-snail shell, castor oil-crab shell and castor oil-egg shell biodiesel products respectively. All three castor oil biodiesel products were produced at various specifications or reaction conditions lettered from A – I usually written as a subscript after the biodiesel product and as a result, 27 samples of biodiesel was produced. The optimal conditions required for the production of the biodiesel were obtained and the fuel properties of all 27 samples of biodiesel produced were determined. The crude castor oil gave acid value and FFA of 5.87mgKOH/g and 3.25 respectively which were above the ASTM standards at 0.4 – 4 mgKOH/g and 0.2 – 2 respectively. The highest surface area was produced from calcined/impregnated crab shell at 170.21 m^2/g. The result from the FTIR analysis showed the presence of O – C – O and O – H bonds in the uncalcined spectra and a strong S ═ O bond after calcination/impregnation. Castor oil-egg shell biodiesel product obtained with H-specification (CE_H) produced the highest biodiesel yield of 95.3 %. This was obtained at optimal conditions of 1:12 oil to methanol ratio, 5 wt% catalyst loading, 60 ^{O}C reaction temperature for 60 min reaction time. Results from the characterization of biodiesel products obtained showed 70, 9.80 mm^2/s and 945 kg/m^3 as maximum values of cetane number, kinematic viscosity and density traced from castor oil-egg shell biodiesel product obtained with H-specification (CE_H), castor oil-snail shell biodiesel product obtained with A-specification (CS_A) and castor oil-egg shell biodiesel products obtained with A-specification (CE_A) respectively.

Keywords: Transesterification, Heterogeneous, Catalysts, Wet-Impregnation

I. Introduction

With lots of developing countries depending directly or indirectly on energy being the principal propeller of a booming economy and social advancement, hike in the cost of fossil fuel and certain environmental adverse effect such as the increase in the average temperature of the earth, emission of detrimental air stressors and greenhouse gases among others will continuously result in the threats the 21st century is being confronted with. This can be attributed to the endless rise in global population and world energy demand. However, this source is insubstantial and will be used up in subsequent time [1].

Studies has relayed that among the green energy technologies listed above, bio-energy has proven to be more reliable as energy produced from plants can be captured and stored thereby providing a more cost effective economic approach and no detrimental threat to humans and the environment [2]. Irrespective of the jeopardy created by the use of fossil fuel for energy generation, the use of biodiesel as a surrogate for fossil fuel replacement till date still remains almost impossible. [3,4]. It is with the above listed setbacks that this waste to energy investigation process is relayed on as the possibility and the effectiveness of utilizing waste derived solid catalyst in the presence of non-edible feedstock's in the production of biodiesel is determined.

Homogeneous catalysts are effective but the set-backs associated with them such as; high energy consumption, wastewater treatment due to unreacted chemicals among others has qualified the use of heterogeneous catalyst especially the CaO –base catalyst [5]. However, in some catalysts, particularly CaO, leaching takes place that adversely influences the reaction [6,7]. Therefore, charging a heterogeneous base catalyst by wet impregnation can help to design and modify the catalyst's surface to meet the requirements of specific applications and solve the issues associated with the use of homogeneous as well as heterogeneous catalyst [8]. This can be achieved to build a CaO catalyst with both acidic and basic reactive sites with zero limitations as there is total involvement of both internal and external surface active species in the reaction [9]. The use of edible vegetable oil results in competition between the food and fuel oil market and as such, triggers a hike in the cost of purchase of vegetable oil and biodiesel. With zero competition, easy accessibility and unique adaptive features, castor oil has been found worthy, attractive and attainable by researchers and energy enthusiasts to be used as a surrogate in place of edible oil [10]. Therefore the aim of this study is to carry out transesterification of

ISSN 2278-2540 | DOI: 10.51583/IJLTEMAS | Volume XIII, Issue V, May 2024

castor oil using H_2SO_4 wet-impregnated crab, egg and snail shell. Optimization was carried out to determine the best reaction conditions that supports the production of a high biodiesel yield.

II. Materials and Methods

2.1. Materials

Separating funnel, reflux condenser, muffle furnace, desiccators, water bath, soxhlet extractor, centrifuge, retort stand, conical flasks, beakers, pipette & burette, magnetic stirrer heating mantle, thermocouple, 500 mL round bottom 3 neck glass reactor. Scanning electron microscope (SEM), x-ray diffraction (XRD), fourier transform infrared radiation (FTIR), x-ray fluorescence spectroscopy (XRF), gas chromatography-mass spectroscopy (GC-MS), Brunauer-Emmett-Teller (BET).

2.2. Reagents

All reagents used in this study were all of analytical grade; ethyl alcohol, chloroform, potassium iodide solution, hanus solution, isopropyl alcohol, n- hexane, methanol, tetraoxosulphate (VI) acid, potassium hydroxide, phenolphthalein indicator, hydrochloric acid,

2.3 Methods

2.3.1 Sample Collection

The castor seeds were brought in bags from a major castor seed dealer. The egg shell was collected from a campus restaurant in Yabatech, Lagos State. While the crab shells were collected at bariga market, Lagos State. The snail shells were collected from a dumpsite at the popular mile one market.

2.3.2 Sample Pretreatment

2.3.2.1 Catalyst pretreatment

The catalysts were pretreated by means of calcination, impregnation and recalcination. Firstly, the shells were brought in and washed thoroughly with warm water to remove impurities and organic matter present in them. To ensure they are completely dried, they were placed in an oven at 105 ^{O}C for 24 hr. With the aim of increasing the surface area, the shells were blended separately and sieved in a 60 mesh size sieve to properly separate the crystals from the fine particles. The egg and crab shells were calcined at 900 ^{O}C for 2 hr while the snail shell was calcined at 800 ^{O}C for 4 hr. For the impregnation process, 500 ml H_2SO_4 was added in drops to 100 g of each of the calcined catalysts with simultaneous stirring, the mixture was stirred with magnetic stirrer for 6 hr and placed in an oven to dry at 105 ^{O}C for 24 hr. Lastly, the egg and crab shells were recalcined at 900 ^{O}C for another 2 hr and the snail shell at 800 ^{O}C for 2 hr.

2.3.2.2 Catalyst Identification

The pattern of identifying the catalyst after pretreatment is shown in table 2.1 below;

Table 2.1: Identification of Catalysts after Pretreatment

Catalysts	Uncalcined Catalysts	Calcined Catalysts	Calcined/Impregnated Catalysts
Snail Shell	S	CS_{800^oC}	CS_{800^oC}/H_2SO_4
Crab Shell	C	$CC_{900\ ^oC}$	$CC_{900\ ^oC}/H_2SO_4$
Egg Shell	E	$CE_{900\ ^oC}$	$CE_{900\ ^oC}/H_2SO_4$

2.3.2.2 Oil Pretreatment

The castor seeds were washed thoroughly with distilled water and sundried for 48 hr. With the aim of deshelling, they were cracked to remove the shells from the seeds. The white seeds were placed in an oven at 90 ^{O}C for 45 minutes and on cooling, they were crushed and placed in a thimble for soxhlet extraction of the oil from the seeds.

2.3.3 Sample Characterization

Both the uncalcined and the calcined/impregnated crab, snail and egg shell catalysts were characterized using various analytical instruments such as; BET, XRF, SEM, FTIR and XRD while the castor oil was subjected to physiochemical analysis and also characterized using GC-MS to quantitatively determine the free fatty acid present in them.

2.3.4 Esterification and Transesterification Processes

A feedstock shown to have a high FFA is first subjected to acid esterification were it is being catalyzed by an acid. About 0.14 ml of H_2SO_4 is added into a conical flask containing 55 ml of methanol. The mixture is heated in a water bath to attain a temperature of 60 ^{O}C. On the other hand, 100 g of the crude feedstock is also weighed accurately into the glass reactor and heated to attain same temperature. Upon attaining that temperature, the content of the conical flask is emptied into the glass reactor and heated at 60 ^{O}C with stirring at a speed of 800 rpm for 1 hr. On cooling, it is placed in a separatory funnel and the esterified oil recovered. For the

ISSN 2278-2540 | DOI: 10.51583/IJLTEMAS | Volume XIII, Issue V, May 2024

transesterification process, a known weight percent of the catalyst is weighed accurately into a known volume of methanol and heated to attain a temperature of 55 ^{O}C while on the other hand, 100 g of the esterified oil is also weighed into the glass reactor and heated to attain same temperature. The content of the conical flask is again emptied into the glass reacted and heated for 1 hr at a 300 rpm stirring speed. The biodiesel produced is separated from the layer of catalyst, glycerol and methanol in a separatory funnel, centrifuged and wet washed with warm water. Its percentage yield is determined by;

% Biodiesel Yield = (Weight of biodiesel/Weight of esterified oil) × 100

The biodiesel produced was characterized according to the various methods proposed by the ASTM standards.

III. Result and Discussion

Table 3.1. Physiochemical Evaluation of Castor oil

Properties	Units	ASTM Value	Castor Oil Values
Moisture content	%	0.05	0.5
Acid value	mgKOH/g	0.4 – 4	5.87
Saponification value	mgKOH/g	175 – 187	195.81
Iodine value	mgI_2/100g	82 – 88	86.50
Free fatty acid	-	0.2 – 2	3.25
Density	g/ml	-	0.972
Viscosity at 40 ^{O}C	mm^2/sec	0.957 – 0.968	170.41

As seen from table 3.1 above, all values obtained were higher than that of the ASTM standard value with exception to iodine value. The high acid value as well as moisture content can be attributed to poor seed handling from processing to harvesting. While the presence of OH and double bond in the ricinoleic structure of the castor oil can initiate both oxidation and hydrolysis thereby increasing the FFA content of the oil. This is answerable to the compulsory subjection of the crude castor oil to esterification before the main transesterification process.

3.1 Characterization of the Uncalcined and Calcined/Impregnated Snail, Crab and Egg Shell

The results obtained from the BET analysis to determine the surface area, pore volume as well as the pore diameter of the catalysts are analyzed in table 3.2 below;

Table 3.2. BET Analysis of Catalyst Samples

Catalysts	Surface Area (m^2/g)	Pore Volume (cm^3/g)	Pore Size (Å)
Uncalcined snail shell	3.80	0.0062	2.015
Calcined snail shell/H_2SO_4 (CS_{800^oC}/H_2SO_4)	2.60	3.461	2.513
Uncalcined egg shell	3.260	2.580	2.105
Calcined egg shell/H_2SO_4 (CS_{800^oC}/H_2SO_4)	3.925	5.50	2.621
Uncalcined crab shell	9.78	0.03	2.46
Calcined crab shell/H_2SO_4 (CS_{800^oC}/H_2SO_4)	170.21	2.08	5.84

From the BET result obtained, it can be deduced that all calcined/impregnated catalyst samples produced higher values for surface areas, pore volumes and pore sizes as compared to their uncalcined counterparts but with exception to calcined/impregnated snail shell with a surface area of 2.60 m^2/g lower than that of its uncalcined state. This can be attributed to the filling of the CaO pores with $CaSO_4$ owing to the long calcination temperature applied.

ISSN 2278-2540 | DOI: 10.51583/IJLTEMAS | Volume XIII, Issue V, May 2024

3.1.1. SEM Analysis of Uncalcined and Calcined/impregnated Samples

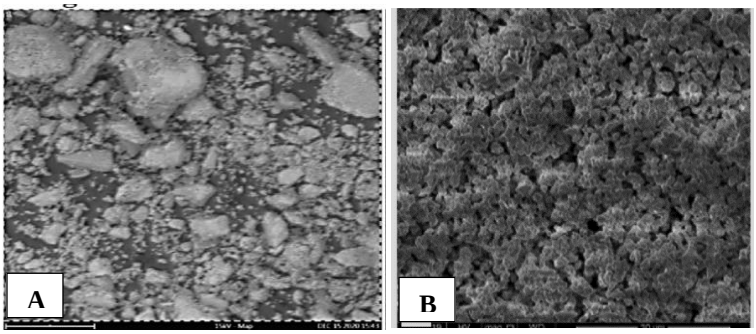

A = Uncalcined B= Calcined/impregnated

Figure 3.1: SEM Image of Uncalcined and Calcined/ Impregnated Crab Shell

The SEM image of the uncalcined and calcined/impregnated crab shell revealed that for the calcined and impregnated shell, there is a distortion in the surface of the catalyst owing to the evaporation of the volatile phases from the surface of the catalysts. However, this distortion led to an increase in its porosity, micropores and mesopores. Whereas in the case of the uncalcined crab shell, there is an uneven arrangement of spherical structural particles with varying sizes and shapes.

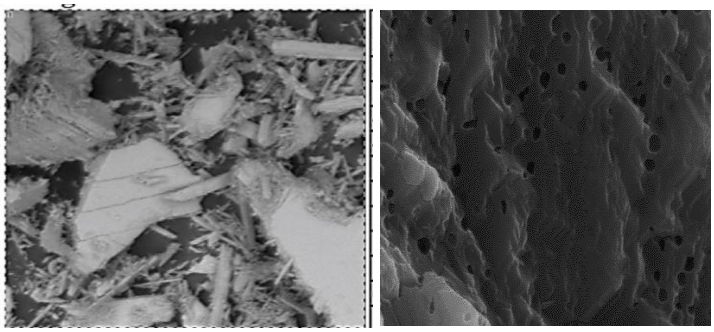

A = Uncalcined B= Calcined/impregnated

Figure 3.2: SEM Image of Uncalcined and Calcined/ Impregnated Snail Shell

As seen from figure 3.2 above, upon calcination and impregnation, there is a well-structured arrangement which showed increase in the porosity of the shell. While among all uncalcined and impregnated samples analyzed, only the uncalcined snail shell catalysts displayed a rod-like structural particle owing to the low values of surface area, pore volume and pore size it possesses as seen from the BET analysis reported. However, same structural pattern was also affirmed by [11].

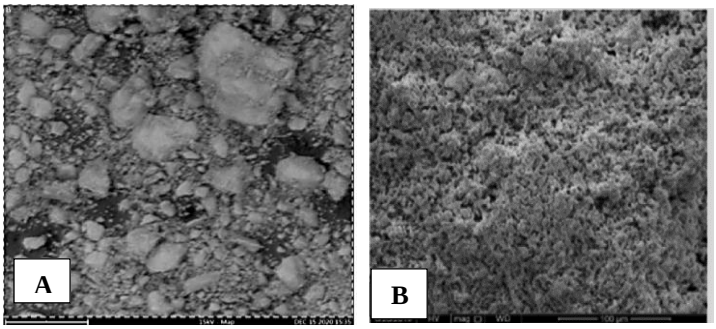

A = Uncalcined B= Calcined/impregnated

Figure 3.3: SEM Image of Uncalcined and Calcined/ Impregnated Egg Shell

The result obtained above shows that the uncalcined egg shell showed an uneven distribution as well as an unstructured arrangement of spherical-shaped particles of various sizes while that of the calcined and impregnated shell shows slight disorderliness in the surface of the catalyst owing to the loss of H_2O and CO_2 from the surface of the catalyst which builds up the concentration of CaO after all the $CaCO_3$ has been successfully removed by means of thermal decomposition.

3.1.2. XRF Analysis of Uncalcined and Calcined/Impregnated Catalysts

The results of the XRF analysis of the uncalcined as well as calcined and impregnated crab, snail and egg shell is summarized and discussed below;

ISSN 2278-2540 | DOI: 10.51583/IJLTEMAS | Volume XIII, Issue V, May 2024

Table 3.3: XRF Results of Uncalcined and Calcined/Impregnated Snail Shell

Element	Atomic Conc. Uncalcined Snail Shell	Weight Conc. Uncalcined Snail Shell	Atomic Conc. $CS_{900}{}^{O}{}_{C}/H_2SO_4$	Weight Conc. $CS_{900}{}^{O}{}_{C}/H_2SO_4$
Ca	90.70	89.52	89.38	88.57
Y	0.92	2.02	0.96	2.10
Ag	0.73	1.94	0.75	1.99
Nb	0.54	1.23	0.66	1.52
K	1.21	1.16	1.30	1.25
Cl	0.86	0.75	1.06	0.93
S	0.88	0.70	57.93	55.32

The XRF results displayed above delineates that calcium remained the most dominant element in all uncalcined and calcined/impregnated catalyst samples. The result for uncalcined and calcined/impregnated snail shell sample as seen from table 3.3 above shows the very low concentration of sulphur obtained before calcination and its high concentration attained after calcination/impregnation can be attributed to the charging of H_2SO_4 into the catalyst after wet impregnation. While the high atomic concentration of calcium in the uncalcined catalyst decreased after calcination and impregnation because the recalcination temperature applied in the catalyst gradually decomposes all the volatile phases in the catalyst thereby building up the concentration of calcium in the catalyst.

Table 3.4: XRF Result of Uncalcined and Calcined Egg Shell

Elements	Atomic Conc. Uncalcined Egg Shell	Weight Conc. Uncalcined Egg Shell	Atomic Conc. $CE_{900}{}^{o}{}_{C}/H_2SO_4$	Weight Conc. $CE_{900}{}^{o}{}_{C}/H_2SO_4$
Ca	85.38	85.55	88.84	89.35
Y	1.03	2.29	0.88	1.94
Al	3.38	2.28	0.99	0.67
Ag	0.83	2.23	0.78	2.08
Ni	0.75	1.74	0.60	1.38
K	1.47	1.44	1.37	1.33
S	1.47	1.18	64.30	61.80

The XRF results displayed in table 3.4 above also depicts that calcium still remained the most dominant element in all uncalcined and calcined/impregnated catalyst samples. The high atomic concentration of calcium obtained from their uncalcined state even became higher after calcination and impregnation. This can be attributed to the high calcination temperature of 900 ^{O}C which initiated the evaporation of the volatile components from the surface of the $CaCO_3$ thereby leading to the increase in the concentration of calcium in the catalyst. Whereas the concentration of sulphur moved from almost not been detected in the uncalcined states to attaining a high atomic concentration after calcination and impregnation. This is answerable to the gradual fading away of the $CaCO_3$ which led to the buildup of the sulphur in the catalyst.

Table 3.5: XRF Results of Uncalcined and Calcined/Impregnated Crab Shell

Elements	Atomic Conc. Uncalcined Crab Shell	Weight Conc. Uncalcined Crab Shell	Atomic Conc. CC_{900OC}/H_2SO_4	Weight Conc. CC_{900OC}/H_2SO_4
Ca	79.54	81.94	85.05	87.82
P	4.38	3.49	4.08	3.26
Y	0.70	1.93	0.74	1.68
Ni	2.20	0.38	0.29	0.69
C	40.33	21.30	26.50	24.54

ISSN 2278-2540 | DOI: 10.51583/IJLTEMAS | Volume XIII, Issue V, May 2024

S	4.19	1.29	66.70	61.58
O	48.32	44.28	53.97	50.87

The XRF results for uncalcined and calcined/impregnated crab shell displayed in table 3.5 above shows that after calcination/impregnation, elements such as calcium, sulphur and oxygen attained higher atomic concentration values of 85.05, 66.70 and 53.97 respectively while other elements such as yitrium, Niobium and phosphorus were seen to be present but at very low concentrations.

3.1.3 XRD Analysis of Uncalcined and Calcined/Impregnated Catalysts

The results of the XRD analysis determined for both the uncalcined as well as calcined/impregnated crab, egg and snail shell catalysts is summarized and discussed below;

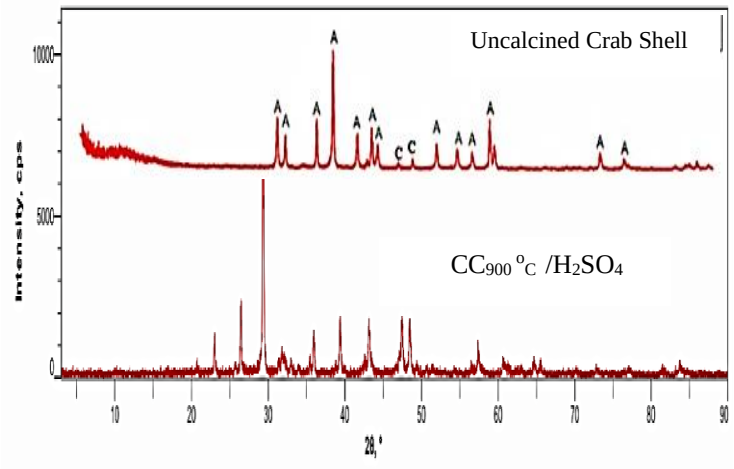

Figure 3.4: XRD Pattern for Uncalcined and Calcined/Impregnated Crab Shell

The spectrum representation of the XRD result of uncalcined crab shell shows the presence of both aragonite and calcite crystalline phases. Figure 3.4 above, clearly shows that the uncalcined crab shell catalyst produced trace amount of calcite but was largely dominated by the aragonite crystal phase at a 2θ range of 26.103 ^{O}, 32.398 ^{O} and 34.013 ^{O}. For the impregnated and calcined crab shell, a 2θ range presented general diffraction peaks at 23.00^{O}, 26.41 ^{O}, 29.30 ^{O}, 39.33 ^{O}, 43.09 ^{O}, 47.40 ^{O}, 48.40 ^{O}. The crystallization of the calcite $CaCO_3$ in crab shell at the initial stage of calcination displays very strong diffraction peaks at 29.33 ^{O}, 35.92 ^{O}, 39.34 ^{O}, 43.09 ^{O}, 47.36 ^{O} and 48.39 ^{O}.

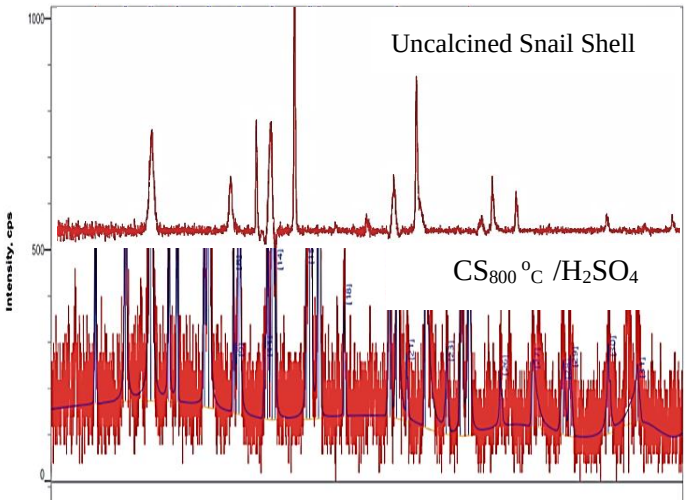

Figure 3.5: XRD Pattern for Uncalcined and Calcined/Impregnated Snail Shell

The result revealed that the crystalline nature of the uncalcined snail shell was that of the aragonite $CaCO_3$ phase which was the most dominating phase produced. This was observed at the theta range of 23.36 °, 34.22 °37.19 °, 38.16 ° and 44.22 °. The spectrum displayed by the calcined/impregnated snail shell catalyst showed very rough diffraction peaks. The qualitative result of the analysis was determined using the phase data view which showed the various phases produced by the spectrum.

ISSN 2278-2540 | DOI: 10.51583/IJLTEMAS | Volume XIII, Issue V, May 2024

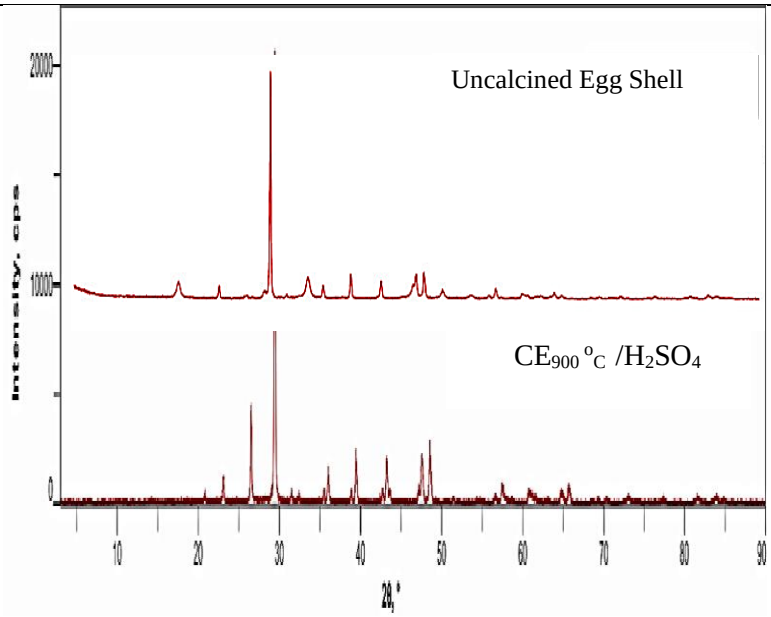

Figure 3.6: XRD Pattern for Uncalcined and Calcined/Impregnated Egg Shell

For the calcined/impregnated egg shell, sharp and intense peak of 29.40 was revealed which connotes the presence of the trigonal crystalline phase of the calcite. This further depicts the disappearance of calcite $CaCO_3$ and the emergence of CaO. While others were reported at 31.43 ^{O}, 35.98 ^{O}, 39.42 ^{O}, 57.42^{O}. The x-ray diffraction patterns obtained for the calcined and uncalcined eggshell particles shows diffraction peaks which suggested a crystalline phase of the main material calcium carbonate in the form of calcite ($CaCO_3$). The major intense peak was traced at a 2θ angle of 27.2° while 22.2°, 30.5°, 37.1°, 36.6°, 41.9°, 46.9°, and 47.7° were minor peaks discovered.

3.1.4 FTIR Analysis of Uncalcined and Calcined/Impregnated Catalysts

The results of the FTIR analysis determined for both the uncalcined as well as calcined/impregnated crab, egg and snail shell catalysts is summarized and discussed below;

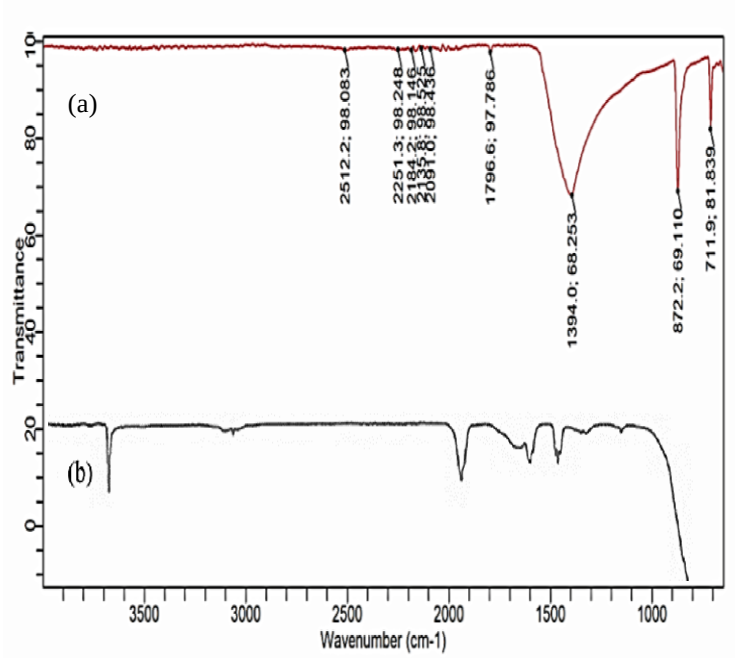

(a) Calcined/impregnated snail shell (b) Uncalcined snail shell

Figure 3.7: FTIR Analysis for Uncalcined and Calcined/Impregnated Snail Shell

For the uncalcined snail shell, the sharp and intense infrared band was attained at 1750 cm^{-1} which shows the presence of asymmetry stretching vibration of the O–C–O bond thereby communicating the presence of CO_3^{-2} present in the catalyst. For the snail shell impregnated and calcined at 800 ^{O}C ($CS_{800}{}^{o}C/H_2SO_4$), a major absorption band of 1304 cm^{-1} was also spotted which also shows the complete thermal decomposition of the $CaSO_4$ to CaO.

ISSN 2278-2540 | DOI: 10.51583/IJLTEMAS | Volume XIII, Issue V, May 2024

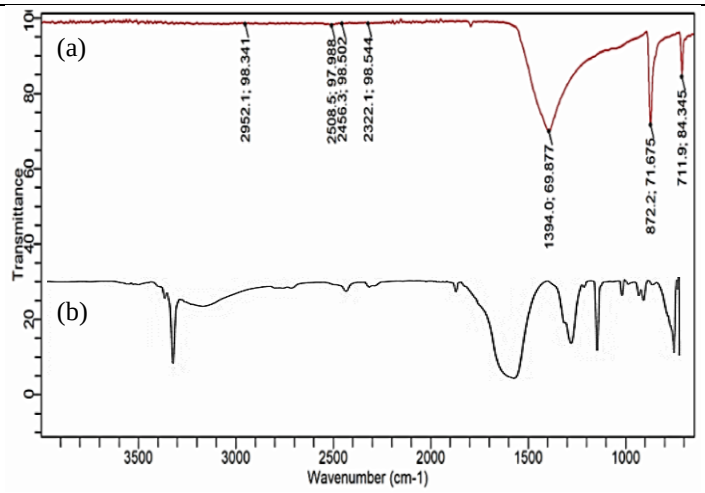

(a) Calcined/impregnated crab shell (b) Uncalcined crab shell

Figure 3.8: FTIR Analysis for Uncalcined and Calcined/Impregnated Crab Shell

As seen in figure 3.8 above, the spectrum of the uncalcined crab shell shows the presence of a sharp peak detected at 1100 cm^{-1} which indicates the stretching vibration of the Ca – O bond. This is answerable to the high atomic and weight concentrations of calcium in the uncalcined crab shell as seen in the XRF result in table 3.5 above. On the other hand, the FTIR spectrum for crab shell impregnated and calcined at 900 ^{O}C ($CC_{900}{}^{o}{}_{C}/H_2SO_4$) revealed an intense infrared band of 1036 cm^{-1} which delineates the presence of asymmetry stretching vibration of a strong S ═ O which signifies the successful thermal dissociation of the sulphite ion from the CaSO4 to give calcium oxide which is the end product [12].

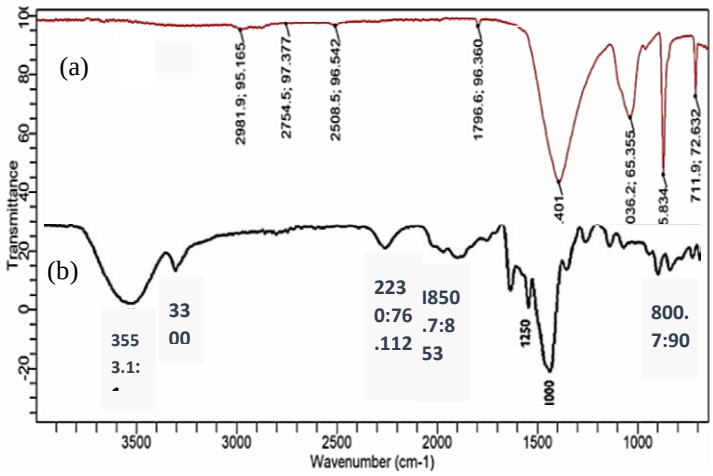

Figure 3.9: FTIR Analysis for Uncalcined and Calcined/Impregnated Egg Shell

The FTIR spectra analysis for uncalcined egg shell revealed the presence of a very wide stretching peak at 3553 cm^{-1} band which connotes the presence of weak stretching vibration of the O – H bond and affirms the presence of gaseous water from the $CaCO_3$. On the other hand, the major absorption band of the egg shell impregnated and calcined at 900 ^{O}C ($CE_{900}{}^{o}{}_{C}/H_2SO_4$) was detected at a peak of 1394 cm^{-1} which depicts the asymmetry stretching vibration of the O–C–O bond.

3.1.5 GC-MS Analysis of Castor Oil

Table 3.6: Percentage Concentration of Free Fatty Acid from Castor oil

Free Fatty Acid Composition	Common Name	Molecular Formula	Concentration (%)
9-Octadecenoic acid	Oleic acid	$C_{18}H_{32}O_2$	5.30
9,12-Octadecadienoic acid	Linoleic acid	$C_{18}H_{31}O_2$	6.10
Octadecanoic acid	Stearic acid	$C_{18}H_{34}O_2$	7.20
Hexadecanoic acid	Palmitic acid	$C_{16}H_{32}O_2$	8.90
12-Hydroxy, 9- Octadecenoic acid	Ricinoleic acid	$C_{18}H_{33}O_3$	72.50

ISSN 2278-2540 | DOI: 10.51583/IJLTEMAS | Volume XIII, Issue V, May 2024

It is observed from the table 3.6 above, ricinoleic acid emerged as the most dominant free fatty acid present at 72.50 % in the oil. With such high percentage concentration, castor oil will continuously maintain its stance as the only prevailing vegetable oil whose fatty acid is embedded with a hydroxyl group at position 12 of the fatty acid chain. Therefore it isn't out of place to conclude that the castor oil used in this research is a highly reactive one because the disappearance of the hydroxyl group paves way for the emergence of the double bond which serves as a reactive channel through which the oil engages in several reactions. Higher ricinoleic value of 84.2 % has also been reported [13].

3.1.6 Characterization of the Biodiesel Produced from Castor Oil

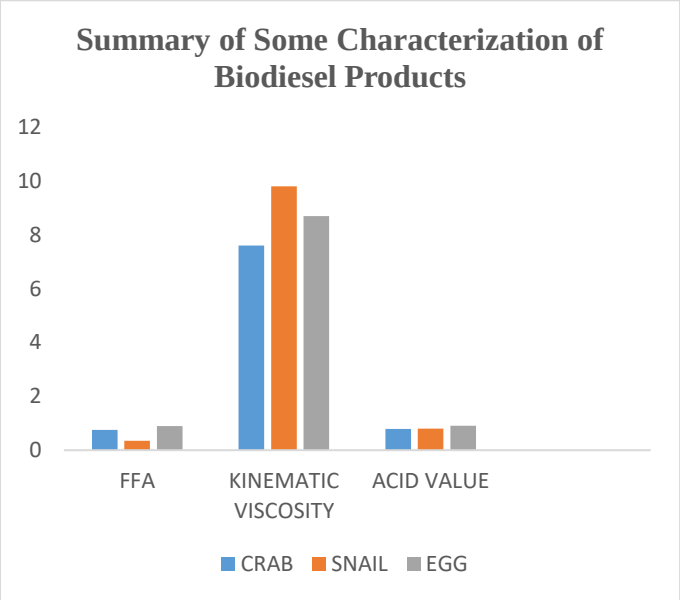

CC, CS and CE = Castor oil crab, snail and egg shell biodiesel products. Subscripts A, C, D, E = various reaction specification as seen from table 3.7 below.

Figure 3.10: Summary of some Characterization of Biodiesel Produced

Figure 3.10 above shows the summary of some fuel properties analyzed in the biodiesel produced. The result showcased some of the biodiesel products with the highest FFA, kinematic viscosity at 40 ^{O}C as well as acid value amongst other properties analyzed obtained from castor oil. The highest FFA value of 0.90 mgKOH/g was produced from CE_C biodiesel product while the highest kinematic viscosity value of 9.80 mm^2/s was spotted from CS_A biodiesel product. Also a value of 0.91 was recorded as the highest acid value traced from CE_C product. All values were higher than the ASTM stipulated standard value while other values are said to fall within the standard value.

3.2 Optimization of Process Parameter for Transesterification Reaction

The optimization process used in this study is governed by the Taguchi Orthogonal array design as seen from the table 3.7 below;

Table 3.7: Array Design of the Effect of Various Reaction Conditions on Castor Oil Egg, Snail and Crab Shell Biodiesel Yields

Reaction Specif.	Oil to Methanol Ratio	Reaction Temp (^{O}C)	Catalyst Loading (wt%)	Reaction Time (min)	Castor Oil Biodiesel
A	1:6	55	1	60	CS_A
B	1:6	60	3	90	CS_B
C	1:6	65	5	120	CS_C
D	1:9	55	1	120	CS_D
E	1:9	60	5	120	CS_E
F	1:9	65	3	60	CS_F
G	1:12	55	3	90	CS_G
H	1:12	60	5	60	CS_H
I	1:12	65	1	90	CS_I

ISSN 2278-2540 | DOI: 10.51583/IJLTEMAS | Volume XIII, Issue V, May 2024

Where A, B, C….I = various reaction specifications for the reaction conditions applied in batches for each of the biodiesel production. CS_A, CS_B …..CS_I = castor oil-snail shell biodiesel products produced using the various reaction specifications.

Table 3.7 above shows the array design governing the transesterification of biodiesel products from castor oil using calcined/impregnated snail shell. This table will be replicated for biodiesel products from calcined/impregnated crab and egg shell making a total of 27 samples of biodiesel produced in the study. The effect of reaction temperature, reaction time, catalyst loading and oil to methanol ratio on the various yields of biodiesel were determined to aid in the optimization process.

3.2.1. Effect of Oil to Methanol Ratio on Biodiesel Yields

Table 3.8: Effect of Oil to Methanol Ratio on the Yields from Castor oil

Oil Methanol Ratio	Reaction Time (min)	Catalyst Loading (wt%)	Reaction Temp. (^OC)	EggShell Biodiesel Product	Snail Shell Biodiesel Products	Crab Shell Biodiesel Products
1:6	60	1	55	CE_A 81.51	CS_A 75.33	CC_A 89.97
1:6	90	3	60	CE_B 83.10	CS_B 89.40	CC_B 90.53
1:6	120	5	65	CE_C 87.50	CS_C 87.10	CC_C 91.26
1:9	120	1	55	CE_D 84.76	CS_D 88.80	CC_D 92.64
1:9	120	5	60	CE_E 89.20	CS_E 84.00	CC_E 83.00
1:9	60	3	65	CE_F 88.00	CS_F 92.70	CC_F 92.77
1:12	90	3	55	CE_G 93.68	CS_G- 93.50	CC_G 90.33
1:12	**60**	**5**	**60**	**CE_H 95.30**	CS_H- 94.20	CC_H 90.11
1:12	90	1	65	CE_I 94.00	CS_I- 86.00	CC_I 90.00

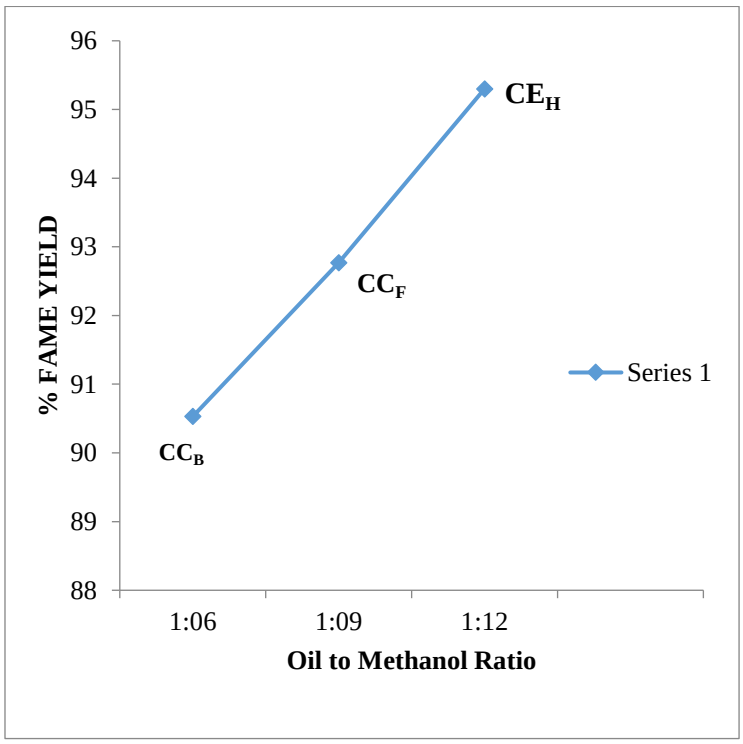

Figure 3.11: Effect of Oil to Methanol ratio on Castor oil --Egg, Snail and Crab shell Biodiesel Yields

From the result obtained in Figure 3.11 above, it can be deduced that the highest biodiesel yield of 95.30 % was obtained at a 1:12 oil to methanol ratio as seen from castor oil egg shell biodiesel product CE_H. The high yield of biodiesel produced can also be attributed to the fact that each mole of biodiesel produced is accounted for every mole of methanol used up in the reaction [14]. While CC_B emerged third with a biodiesel yield of 90.53 % and a 1:6 oil to methanol ratio.

ISSN 2278-2540 | DOI: 10.51583/IJLTEMAS | Volume XIII, Issue V, May 2024

3.2.2. Effect of Catalyst Loading on Biodiesel Yields

Table 3.9: Effect of Catalyst Loading on the Yields from Castor oil

Catalyst Loading (wt%)	Reaction Time (min)	Oil to Methanol Ratio	Reaction Temp. (^{O}C)	EggShell Biodiesel Products		Snail Shell Biodiesel Products		Crab Shell Biodiesel Products	
1	60	1:6	55	CE_A	81.51	CS_A	75.33	CC_A	89.97
1	120	1:9	55	CE_D	84.76	CS_D	88.80	CC_D	92.64
1	90	1:12	65	CE_I	94.00	CS_I	86.00	CC_I	90.00
3	90	1:6	60	CE_B	83.10	CS_B	89.40	CC_B	90.53
3	60	1:9	65	CE_F	88.00	CS_F	92.70	CC_F	92.77
3	90	1:12	55	CE_G	93.68	CS_G	93.50	CC_G	90.33
5	**60**	**1:12**	**60**	**CE_H**	**95.30**	**CS_H**	**94.20**	**CC_H**	**90.11**
5	120	1:6	65	CE_C	87.50	CS_C	87.10	CC_C	91.26
5	120	1:9	60	CE_E	89.20	CS_E	94.20	CC_E	83.00

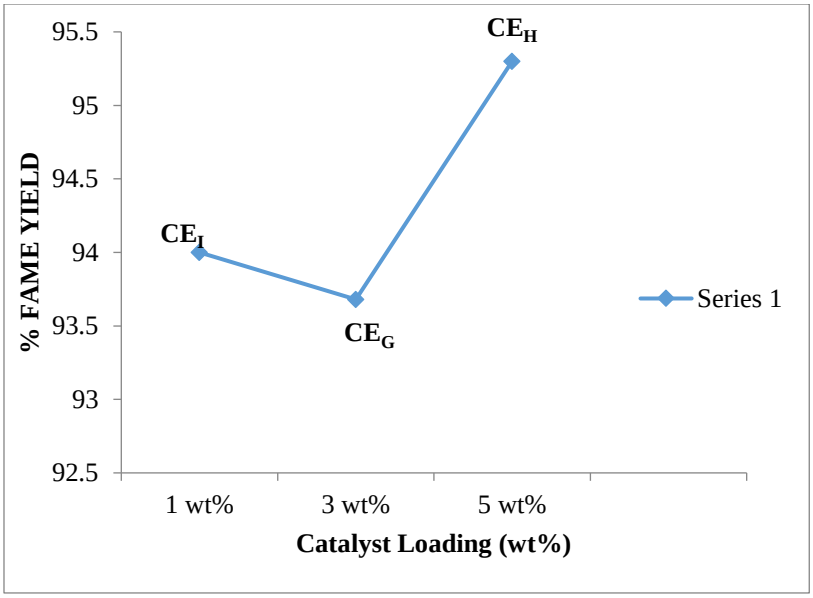

Figure 3.12: Effect of Catalyst Loading on Castor oil -Egg, Snail and Crab shell Biodiesel Yields

The result displayed on figure 3.12 above depicts that among all biodiesel products obtained, castor oil egg shell product CE_H produced the highest yield at 95.30 % at a catalyst loading of 5 wt%. As seen from table 3.7 above, H specification is embodied with a high concentration of the products which are oil and methanol at 1:12. Therefore it can be said that the high product ratio matches the 5 wt% used. This is in agreement with the report communicated by [15] that when the weight of the catalyst greatly outweighs that of the oil and methanol, it creates an imbalance thereby distorting the rate of effective collision. While a slightly low yield of 94.00 % was obtained from castor oil egg shell biodiesel product CE_I at 1 wt% catalyst loading. Also the highest biodiesel yield at 5 wt% catalyst loading accompanied by a temperature of 60 ^{O}C only depicts that a high catalyst loading and temperature increases the enthalpy of the reaction which automatically increases the activation energy of the reaction [16].

3.2.3. Effect of Reaction Time on Biodiesel Yield

Table 3.10: Effect of Reaction Time on Yields from Castor oil

Reaction Timw. (min)	Reaction Temp. (^{O}C)	Catalyst Loading (wt%)	Oil to Methanol Ratio	EggShell Biodiesel Products	Snail Shell Biodiesel Products	Crab Shell Biodiesel Products

ISSN 2278-2540 | DOI: 10.51583/IJLTEMAS | Volume XIII, Issue V, May 2024

60	55	1	1:6	CE_A – 81.51	CS_A- 75.33	CC_A – 89.97
60	**60**	**5**	**1:12**	**CE_H – 95.30**	**CS_H - 94.20**	**CC_H – 90.11**
60	65	3	1:9	CE_F – 88.00	CS_F- 92.70	CC_F – 92.77
90	55	3	1:12	CE_B- 83.10	CS_B- 89.40	CC_B – 90.53
90	60	3	1:6	CE_G – 93.68	CS_G- 93.50	CC_G - 90.33
90	65	1	1:12	CE_I- 94.00	CS_I- 86.00	CC_I – 90.00
120	65	5	1:9	CE_C- 87.50	CS_C- 87.10	CC_C- 91.26
120	55	1	1:9	CE_D- 84.76	CS_D- 88.80	CC_D – 92.64
120	60	5	1:6	CE_E – 89.20	CS_E- 84.00	CC_E– 83.00

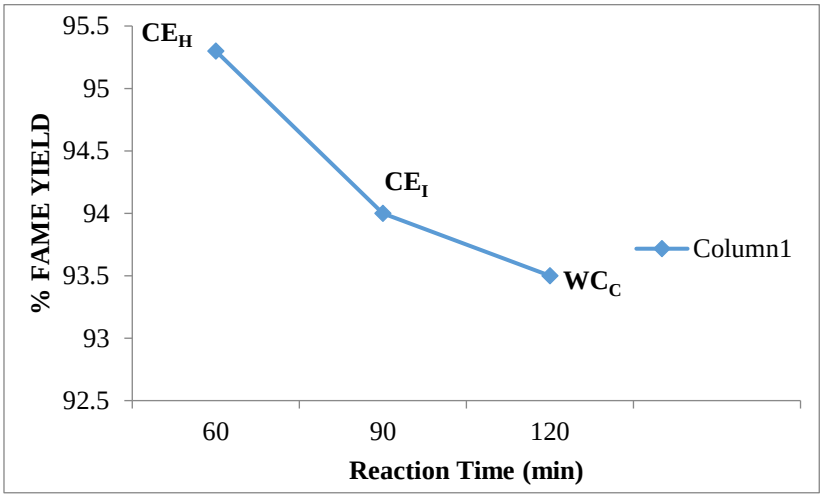

Figure 3.13: Effect of Reaction Time on Castor oil- Egg, Snail and Crab shell Biodiesel Yields

Among all biodiesel samples produced, the highest yield of 95.30 % was obtained from CE_H biodiesel product with a retention time of 60 min as seen from figure 3.13 above. Meanwhile at 94.00 %, castor oil – egg shell biodiesel product CE_I recorded a yield slightly lower than that of CE_H at a retention time of 90 min. Extending the retention time above 90 min would give room for loss of methanol via evaporation thereby decreasing the yield of biodiesel as seen from castor oil crab shell biodiesel product CC_D emerging third with a 92.64 % biodiesel yield at a reaction time of 120 min. Furthermore, at 120 min reaction time, there is an increase in production cost as much amount of energy will be lost in the process of conversion. [17].

3.2.4. Effect of Reaction Temperature on Biodiesel Yield

Table 3.11: Effect of Temperature on Yields from Castor Oil

Reaction Temp. (^OC)	Reaction Time (min)	Catalyst Loading (wt%)	Oil to Methanol Ratio	EggShell Biodiesel Products	Snail Shell Biodiesel Products	Crab Shell Biodiesel Products
55	60	1	1:6	CE_A 81.51	CS_A 75.33	CC_A 89.97
55	90	3	1:9	CE_D 84.76	CS_D 88.80	CC_D 92.64
55	120	3	1:12	CE_G 93.68	CS_G 93.50	CC_G 90.33
60	120	1	1:6	CE_B 83.10	CS_B 89.40	CC_B 90.53
60	120	5	1:9	CE_E 89.20	CS_E 84.00	CC_E 83.00
60	**60**	**5**	**1:12**	**CE_H 95.30**	**CS_H 94.20**	**CC_H 90.11**
65	90	3	1:9	CE_F 88.00	CS_F 92.70	CC_F 90.33
65	60	5	1:6	CE_C 87.50	CS_C 87.10	CC_C 91.26
65	90	1	1:12	CE_I 94.00	CS_I 86.00	CC_I 90.00

ISSN 2278-2540 | DOI: 10.51583/IJLTEMAS | Volume XIII, Issue V, May 2024

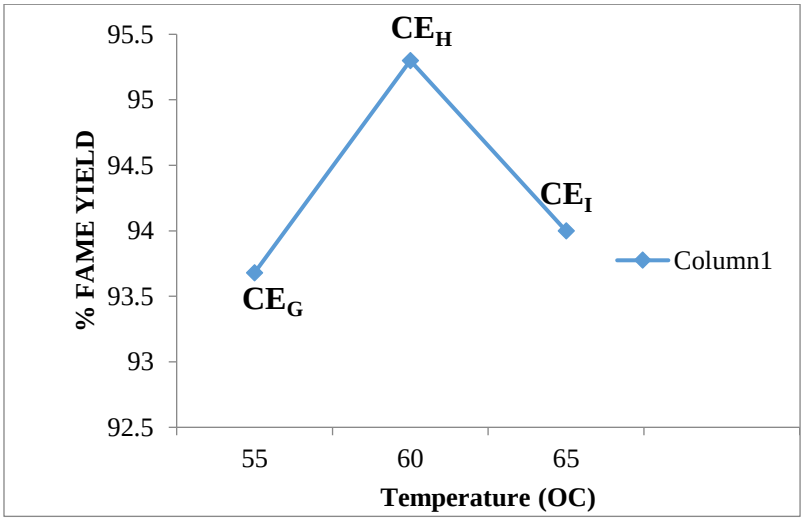

Figure 3.14: Effect of Reaction Temperature on Castor oil- Egg, Snail and Crab shell Biodiesel Yields

The highest biodiesel yield of 95.30 % was produced at a temperature of 60 ^{O}C from CE_H. It is said that the effectiveness of temperature is highly dependent on the surface area provided as seen from calcined/impregnated egg shell in the BET analysis displayed in table 3.2 above. Also at 60 ^{O}C reaction temperature, the temperature was high enough to initiate a translational energy within the molecules of the compound which is said to be equal or even higher than the activation energy. Castor oil egg shell biodiesel product CE_I produced a 94.00% biodiesel yield at a temperature of 65 ^{O}C because a temperature above the boiling point of methanol will decrease the yield of the biodiesel and vice versa [18].

IV. Conclusion

In this study, transesterification of castor oil using H_2SO_4 wet-impregnated crab, egg and snail shell produced various biodiesel yields as seen from figure 4.1 below;

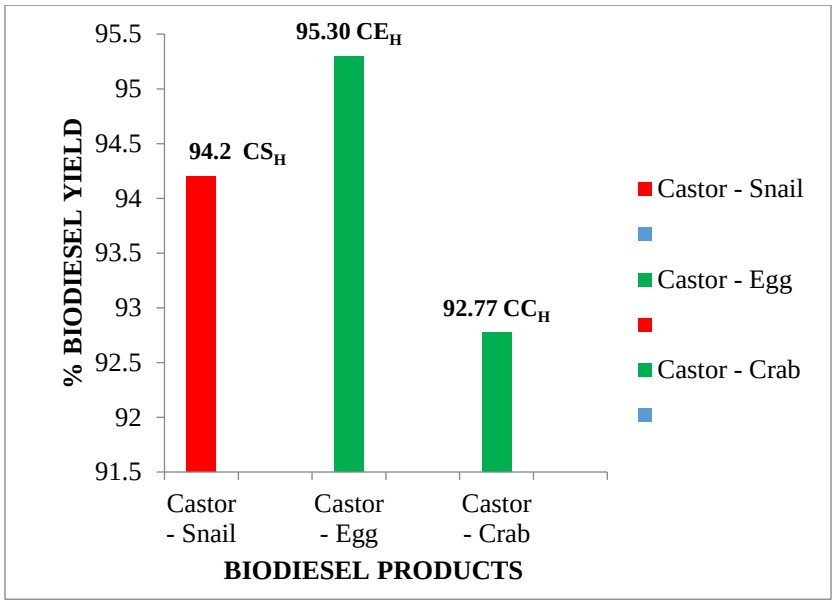

Figure 4.1: Summary of Biodiesel Yields from Castor oil- Snail, Egg and Crab shell Biodiesel Products

From the result displayed above, biodiesel yields of 95.30, 94.20 and 92.77 % were produced from castor oil- egg, snail and crab shell biodiesel products CE_H, CS_H and CC_H respectively. The highest biodiesel yield of 95.30 % was produced from castor oil-egg shell biodiesel product CE_H at optimal conditions of 5 wt%, 1:12, 60 ^{O}C and 60 min as seen from figure 4.1 above.

V. Recommendations

The common problem generally faced by the energy sector and the green energy enthusiasts has and will continue to be the existence of high FFA feedstock's which totally affects biodiesel from its production, utilization as well as its economic stance. Therefore, it is highly recommended that a more dynamic approach be developed in the improvement of the genetic evolution of crop species so as to obtain crops with better varieties and yield. Such crops must possess low FFA while enhancing a high biodiesel yield. Also to discover an appropriate catalyst with high internal and external adsorption and reactivity, capable of annulling all limitations while

ISSN 2278-2540 | DOI: 10.51583/IJLTEMAS | Volume XIII, Issue V, May 2024

promoting high biodiesel yield. Lastly develop a technology for the containing of the CO_2 released after thermal decomposition so as to promote resource recovery as well as greenhouse gas reduction.

References

1. Tsegay B. (2019). Production of Biodiesel from Castor Seed Oil via Transesterification with Methanol-Ethanol Blends Using Calcium Oxide as Catalyst. Chemical and Bioengineering of Addis Ababa Institute of Technology. Chemical and Bio Engineering.
2. Kartika A., Yani M., Ariono D., Evon P., Rigal L. (2013). Biodiesel Production from Jatropha Seeds: Solvent Extraction and In Situ Transesterification in a Single Step. Fuel, 106, 111–117.
3. Coronado C.R., Carvalho J.A.D., Silveira J.L. (2009). Biodiesel CO2 Emissions: A Comparison with the Main Fuels in the Brazilian Market. Fuel Processing Technology, 90, 204-211.
4. Singh V., Yadav M., Sharma Y.C. (2017). Effect of Co-Solvent on Biodiesel Production Using Calcium Aluminium Oxide as a Reusable Catalyst and Waste Vegetable Oil. Fuel, 203, 360-369.
5. Abdulkareem A.S., Uthman H., Afolabi A.S., Awonebe O.L. (2011). Extraction and Optimization of Oil From Moringa Oleifera Seed as an Alternative Feedstock for the Production of Biodiesel. In: Majid N., Mostafa K., editors. Sustainable Growth and Application in Renewable Energy Sources. InTech. pp. 243-268.
6. Sharma S.K., Singh A.P. (2011). Pharmacognostical Evaluation of Roots of Simmondsia chinensis Schneider. International Journal of Pharmaceutical Sciences and Drug Research, 3(4), 323–326.
7. Chakraborty R., Bepari S., Banerjee A. (2011). Application of Calcined Waste Fish (Labeo rohita) Scale as Low-Cost Heterogeneous Catalyst for Biodiesel Synthesis. Bioresource Technology, 102, 3610-3618.
8. Helwani Z., Othman M.R., Aziz N., Kim J., Fernando W.J.N. (2009). Solid Heterogeneous Catalysts in Transesterification of Triglycerides with Methanol: A Review. Applied Catalysis A: General, 363(1), 1–10.
9. Kiss A.A., Dimian A.C., Rothenberg G. (2008). Biodiesel by Catalytic Reactive Distillation Powered by Metal Oxides. Energy & Fuels, 22, 598-604.
10. Laskar I.B., Rajkumari K., Gupta R., Chatterjee S., Paul B., Rokhum L. (2018). Waste Snail Shell Derived Heterogeneous Catalyst for Biodiesel Production by the Transesterification of Soybean Oil. RSC Advances.
11. Hajlari S.A., Najafi B., Ardabili S.F. (2019). Castor Oil, a Source for Biodiesel Production and Its Impact on the Diesel Engine Performance. Reinforced Plastics, 28, 1–10.
12. Kolawole S.A., Zakariyaw A.A., Omoniyi A.O. (2020). Preparation and Characterization of Epoxy Filled Snail Shell Thermoset Composite. Direct Research Journal of Chemistry and Material Science, 6, 8–13.
13. Salimon J., Salih N., Yousif E. (2010). Biolubricants: Raw Materials, Chemical Modifications and Environmental Benefits. European Journal of Lipid Science and Technology, 112(5), 519–530.
14. Hossain A.B.M.S., Mazen M.A. (2010). Effects of Catalyst Types and Concentrations on Biodiesel Production from Waste Soybean Oil Biomass as Renewable Energy and Environmental Recycling Process. Australian Journal of Crop Science, 4(7), 550–555.
15. Kolawole S.A., Zakariyaw A.A., Omoniyi A.O. (2020). Preparation and Characterization of Epoxy Filled Snail Shell Thermoset Composite. Direct Research Journal of Chemistry and Material Science, 6, 8–13.
16. Nageswara R.L., Hassan S.T. (2018). Utilization of Modified Egg Shells as Solid Catalyst for the Conversion of Waste Cooking Oil to Biodiesel. Department of Mechanical and Industrial Engineering, Caledonian College of Engineering.
17. Hameed B.H., Lai L.F., Chin L.H. (2009). Production of Biodiesel from Palm Oil (Elaeis guineensis) Using Heterogeneous Catalyst: An Optimized Process. Fuel Processing Technology, 90, 606-610.
18. Kumar V.S., Navaratnam V. (2013). Neem (Azadirachta indica): Prehistory to Contemporary Medicinal Uses to Humankind. Asian Pacific Journal of Tropical Biomedicine, 3(7), 505-514.